29th International Cosmic Ray Conference Pune (2005) **10**, 227-242

The Milagro Gamma-Ray Observatory

A.J. Smith for the Milagro Collaboration
University of Maryland, College Park, MD 20742-4111
Presenter: Andrew Smith (asmith@umdgrb.umd.edu)

Milagro is a unique water Cherenkov detector designed for very high energy (VHE) gamma-ray astronomy. The water Cherenkov technique gives Milagro an unprecedented sensitivity and energy threshold. A deep detector layer is used to identify penetrating particles (muons and hadrons) present in hadron induced showers allowing for the rejection of backgrounds which substantially increases sensitivity. This paper describes the Milagro detector, its mode of operation and sensitivity to gamma-ray sources. Recent results of Milagro are presented including the recent detection of diffuses gamma-ray emission from the Galactic plane and the Cygnus region, search for VHE radiation from gamma-ray bursts and a survey of the northern sky for gamma-ray sources.

1. Introduction

Milagro is a water Cherenkov extensive air-shower detector designed for high-energy gamma-ray astronomy to understand the most extreme environments in the universe and to utilize the beams of gamma rays from these distant sources to further our understanding of high energy astrophysics. Milagro's wide field of view, good hadron rejection, high duty cycle, and large area make it complementary to other forefront high energy gamma ray detectors.

Atmospheric Cherenkov telescopes (ACTs) such as VERITAS [1,2], MAGIC [3,4] and HESS [5] have shown us that there are many sources[6] of TeV gamma rays including plerions, supernova remnants, super-massive black holes (e.g. in active galactic nuclei), pulsar wind nebulae, micro-quasars and molecular clouds. Some of these sources appear from earth to be point-like. Others are clearly extended. Some are highly variable while many appear steady. The nature of the spectra also varies from hard to soft.

Satellite experiments such as BATSE[7], HETE-2[8] and now Swift[9], which are sensitive in the keV to MeV range, have explored gamma-ray bursts (GRBs) which may be the most energetic phenomenon in the universe. No cutoff has been observed and leading models predict a TeV component [10]. Gamma rays are also produced when high-energy cosmic rays interact with matter in our galaxy producing diffuse high energy gamma rays. EGRET [11] showed a bright diffuse glow of >100 MeV photons from the galactic plane. Other potential sources include more exotic objects (which may or may not be detectable) such as evaporating primordial black holes, topological defects, and dark matter particle annihilation and decay [12]. The gamma rays from distant sources interact with the ambient photon fields in the universe as they travel to earth. By measuring the effects of these interactions on gamma ray spectra we can understand the nature of the fields that pervade the universe.

The ideal environment for gamma-ray astronomy is in space where the primary gamma ray can be stopped and contained within a calorimeter and backgrounds from charged hadrons and electrons can be easily vetoed. The EGRET instrument on the Compton Gamma-Ray Observatory (CGRO) could detect gamma-rays with energies up to ~30 GeV. The principle limitation of space based gamma ray telescopes is their small geometrical factor; the effective area of EGRET was only ~0.01 m^2. The GLAST [13] telescope, scheduled for launch in late 2007, will be much more sensitive than its predecessors, but still only have an effective collection area of ~0.1 m^2. This collection area limits the sensitivity for space based instruments to high energy gamma rays. In contrast, ground based VHE gamma-ray detectors typically have effective areas that range up to 10^4 to 10^5 m^2, this is because the region of influence of a single gamma ray is amplified by

the shower it produces in the atmosphere and it is possible to build vary large detectors on the ground and take advantage of the broad lateral extent of air shower particle to detect a gamma-ray primary even if the core does not land on the detector. Ground based detectors are capable of making very sensitive measurements of high energy emission from sources with fluxes that satellite instruments are too small to detect.

The excellent flux sensitivity of ACT's for detection of gamma-ray point sources is achieved through large effective area, low energy threshold, good background (hadron) rejection and excellent angular resolution. Similarly, Milagro has a large effective area and good background rejection, but has a lower instantaneous sensitivity because of its higher threshold and its angular resolution is ~0.5^o compared with ~<0.1^o for ACTs. The angular resolution and sensitivity of ACTs make them ideal to study steady VHE emission as well as short-term flaring from known sources. However, ACTs can only be used on clear, dark nights, and have a relatively narrow field of view, ~4^o. Thus they are not well suited to perform sky surveys, monitor transient sources for episodic emission, search for transient emission from a source at an unknown direction (such as from a GRB), or to probe structures which are larger than their field of view. In contrast, Milagro can operate 24 hours per day, regardless of weather, and can observe the entire overhead sky; an EAS-array is able to continuously observe every source in its field of view, every day of the year.

Previous EAS scintillation arrays have been sensitive to showers above 10's of TeV. Milagro is the first EAS detector which has a peak sensitivity near 1 TeV. Only the Tibet air shower array, located at an extremely high altitude of ~4300m, has a threshold near that of Milagro. The ARGO array, currently under construction will rival Milagro's sensitivity, but both ARGO and Tibet lack the ability to reject hadronic backgrounds. The vastly superior aperture and exposure of the EAS-arrays makes them ideal instruments for the study and potentially discovery of TeV gamma rays from GRBs and other transient sources in VHE gamma-rays. With Milagro we continuously monitor the entire overhead sky for transient (with durations as short as 1 millisecond) and steady sources of TeV gamma rays.

VHE gamma rays are a natural byproduct of most GRB production models and are often predicted to have comparable fluence at TeV and MeV energies [14]. This is due to the fact that the keV-MeV emission from GRBs is likely due to synchrotron radiation produced by highly accelerated electrons within the strong magnetic field of a jet with bulk Lorentz factors exceeding 100. In such an environment, the inverse Compton mechanism for transferring energy from electrons to gamma rays is likely to complement synchrotron radiation and produce a second VHE component of GRB emission with fluence possibly peaked at 1 TeV or beyond. Whether or not the inverse Compton mechanism contributes minimally or even dominates the energy production depends on the environment of the particle acceleration and the gamma-ray production. VHE measurements may be critical to the understanding of gamma-ray production in GRBs, similar to the manner in which the TeV measurements by ACTs have resolved the degeneracy between magnetic field and electron energy in blazers [15]. In addition, GRBs will likely accelerate hadrons--maybe even producing the ultra high energy cosmic rays. Hadrons will create TeV gamma rays via cascades made by photo-pion production. A recent analysis of a GRB detected by EGRET is most easily explained by such a hadronic process [16] with one of the key features being a slower decay of this higher energy flux. Now that Swift is operating Milagro

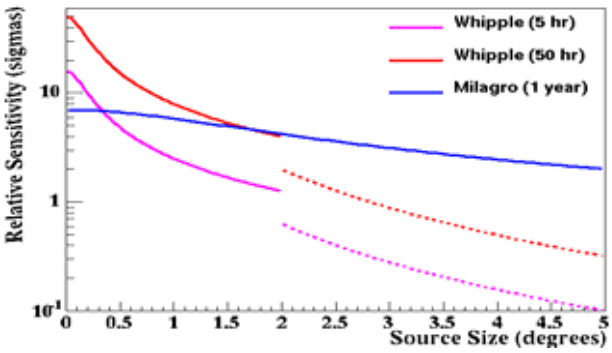

Figure 1 - Relative sensitivity as a function of source size for 1 year of Milagro and Whipple for 5 & 50 hours

will either detect coincident GRBs giving direct measurement of the TeV flux or constrain many GRB models.

ACTs such as VERITAS and HESS are clearly superior for observing known point-like or moderately extended objects. However, as the apparent size of an object approaches or exceeds the field of view of an ACT its sensitively drops significantly. Figure 1 shows a comparison of sensitivity for Milagro and Whipple as a function of source size (diameter) and for different observation periods. It is clear that for a truly extended source such as the galactic plane a detector like Milagro has the advantage. As a result, we have the first clear signal from diffuse TeV gamma-ray emission from the galactic plane as well a highly significant detection of a diffuse source. (These results are presented in this paper). At this point our observations do not allow us to determine whether these diffuse signals are from a collection of point sources or are from gammas from π^o decay resulting from hadronic interactions of the charged cosmic rays with matter. Measuring the spectra of these diffuse sources should allow us to differentiate between these alternatives. Recent improvements to Milagro will allow us to make measurements that have spectral uncertainties of ~0.2 on these sources.

Milagro continuously views the northern sky in the TeV energy range. Our field of view has a substantial overlap with the IceCube neutrino detector [17] being enlarged at the South Pole. IceCube will also monitor the northern sky for transient events such as GRBs. A simultaneous observation of a burst using different particles (gammas and neutrinos) would be much more powerful than one alone.

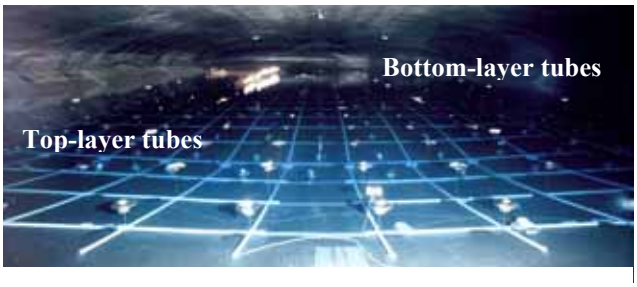

Figure 2- The Milagro pond with the cover inflated for servicing. Both layers of PMTs can be seen floating up from the grid.

Milagro is an experiment that brings together different disciplines. The experiment provides an independent method for measuring the flux of gamma rays seen by ACTs and EAS arrays. It also impacts solar physics. The experiment and its data are also easy to explain to students and the general public, who often have difficulty understanding how we claim to see particles that they don't. The collaboration has been very active in exposing students and the general public to the excitement of the particle astrophysics field.

2. The Milagro Detector

Figure 3 - Aerial photo of Milagro with outrigger array – Red dots show outrigger positions.

Milagro is a water Cherenkov EAS detector located near Los Alamos, NM at 2630m above sea level, consisting of a ~5,000 m^2 central (pond) detector surrounded by an array of 175 instrumented water tanks, (outriggers) that span an area of roughly 40,000 m^2. Unlike scintillation arrays, the Milagro pond densely samples the EAS particles that reach the ground. Since the Cherenkov angle in water is 41^o, an array of photomultiplier tubes (PMTs) placed at a depth of roughly equal to their spacing can detect nearly all of the particles that enter the water. In addition, at ground level the

gamma rays in the EAS outnumber the electrons and positrons by a factor of ~4. Since the PMTs are placed below 4 radiation lengths of water these gamma rays are detected with high efficiency. These features give Milagro an unprecedented energy threshold for an EAS array. A second layer of PMTs under 16 radiation lengths of water is sensitive to the hadronic component of cosmic-ray induced air showers – this is used for background rejection.

The Milagro pond is a 6-million gallon water reservoir, which measures 80m x 60m x 8m deep and is covered with a light-tight cover. The reservoir is instrumented with 723 20-cm PMTs on a 2.8m x 2.8m grid. The PMTs are deployed in two layers. The top layer of 450 PMTs is under 1.5 meters of water and the bottom layer of 273 PMTs is under 6 meters of water. The sides of the reservoir are sloped (2:1) so that the area of the bottom of the reservoir is smaller than the top, leading to the smaller number of PMTs in the bottom layer. The pond interior is shown in Figure 2 and an aerial view is shown in Figure 3.

2.1 Recent Improvements to Milagro

On average the PMTs will detect most electromagnetic particles that enter the pond. This sensitivity allows for the detection of extensive air showers with cores far from the pond (over 100 meters away). The shower front is not a plane, but is curved, therefore, a fitted shower plane using the wrong core position will not be perpendicular to the true direction of the primary particle. This effect tends to degrade the angular resolution of Milagro, especially if the shower core is outside the pond. The outrigger array consists of 175 water tanks surrounding the Milagro pond. Each detector is a 500 gallon water tank with an area of ~4.6m^2 and 1m high. The tanks are lined with Tyvek (to reflect the light produced in the tank) and a PMT looks down into the tank. The tanks are distributed over ~40,000 m^2 around the pond. The array deployment was completed in 2003. Starting in Fall 2004 the calibration system for the outriggers was complete and we fully incorporated the outrigger array into the reconstruction of the core location, angle fit and the background rejection.

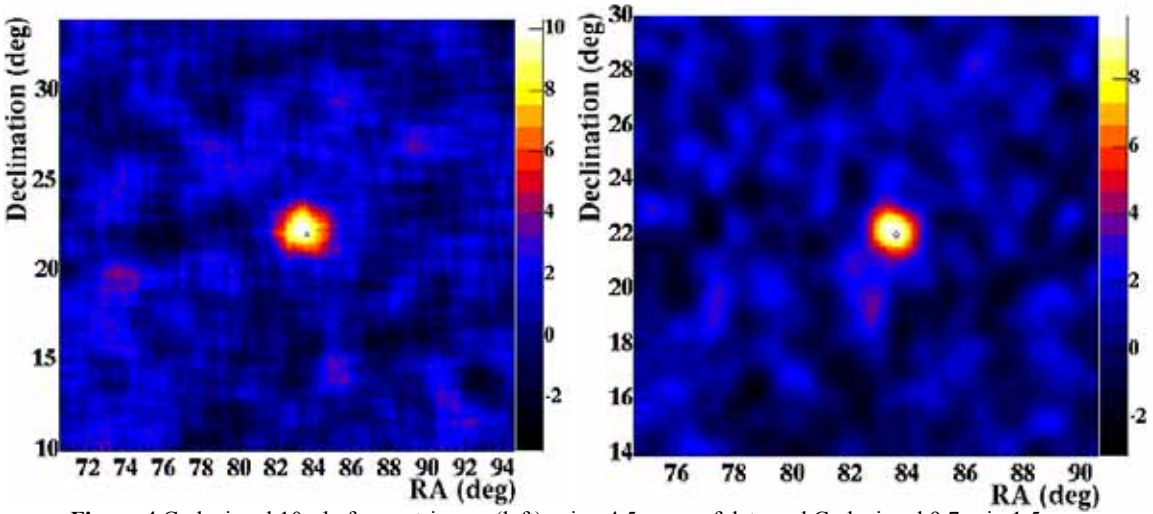

Figure 4 Crab signal 10σ before outriggers (left) using 4.5 years of data and Crab signal 9.7 σ in 1.5 years after outriggers (right – with a smaller scale).

As a result incorporating the outriggers we have made a major improvement in the angular resolution of the detector. Using our initial 4.5 years of data we obtained ~10σ on the Crab (which is the field's standard candle). See Figure 4. With the outriggers we now can obtain approximately the same signal (9.7σ) in just

1.5 years. This improvement is largely due to improving the angular resolution from 0.75° to 0.40°. (Note that the right plot in Figure 4 has a smaller scale showing an improved angular resolution).

2.2 Gamma-Hadron Separation

The hadronic background from cosmic rays can outnumber the gamma rays by a factor of 10,000 to 1 (or more depending upon the angular size of the region examined and the flux of the source). The Whipple collaboration perfected an imaging technique for differentiating between hadronic cosmic rays and gamma-ray induced air showers in an atmospheric Cherenkov telescope [18], thereby launching the present age of high-energy gamma-ray astrophysics. We have developed a technique that uses the information in the bottom layer of Milagro to reject the hadronic background. Hadronic cosmic rays generate air showers that contain penetrating particles, such as muons and hadrons that shower in the water. Such penetrating particles deposit a large amount of light in a small region in the bottom of the detector. An air shower that contains no penetrating particles will illuminate the bottom of the detector with a relatively uniform, low

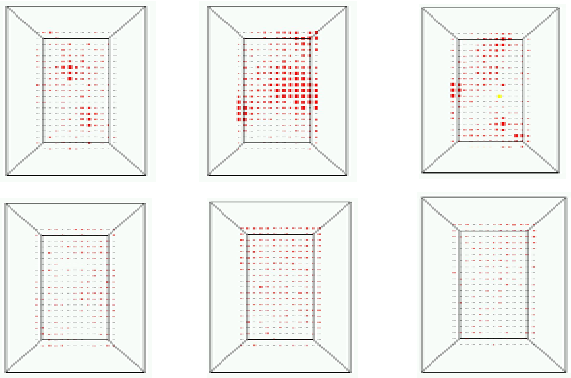

Figure 5. Upper panel shows 3 typical MC proton events and the lower panel shows 3 typical MC gamma-ray induced events as observed in the bottom layer of Milagro. The area of the squares is proportional to the measured pulse height in the PMT.

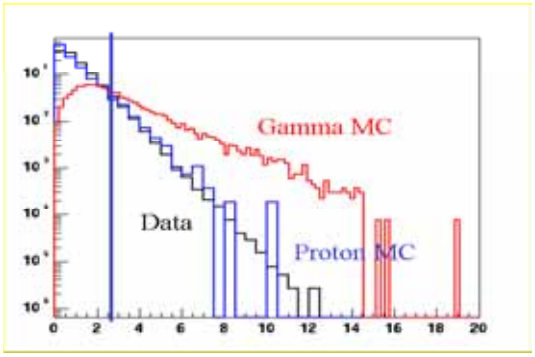

Figure 6. The compactness distribution for data (black curve), Monte Carlo protons (blue), and Monte Carlo gamma rays (red curve). Events to the left of the vertical line are considered background.

level of light containing a single broad peak at the position of the shower core, while a hadron induced shower is almost always accompanied by muons and showering hadrons which can be identified as clumps deposited energy in the deep layer. Figure 5 shows three typical proton and gamma-ray induced events as viewed in the bottom layer of Milagro. Small clumps of light are easily distinguished in the proton-induced events. We have found a simple parameter which is a measure of this clustering, called compactness ($C=N_{PMT}(>2PE)/Pe_{Max}$), that is sensitive to the differences between proton and gamma-ray induced events. The numerator is the number of PMTs in the bottom layer that are struck with more than 2 photoelectrons (PEs) and the denominator is the charge, in PEs, of the brightest PMT in the bottom layer. Penetrating particles that illuminate a small region on the bottom lead to small values of C, while gamma-ray events lead to large values of C. Figure 6 shows the C distribution for cosmic ray and gamma-ray induced events (from simulations) and data. There is good agreement between data and simulations of proton induced events. By rejecting all events with $C<2.5$ we reject 90% of the background events while retaining 50% of the gamma-ray induced events: an improvement in sensitivity (Q value) of 1.6.

With the addition of our outrigger array we now see an overall improved angular resolution, but especially for large showers where previously systematics associated with core error dominated. As a result when we

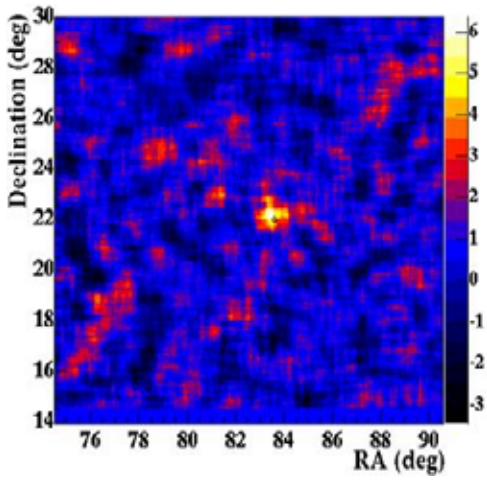

Figure 7. Crab data with C>6 and nfit >200. Signal to background for this data set is ~0.3

make hard cuts (C>6.0) on compactness and the number of counters in the fit (>200) for the Crab we get a reduction in background hadrons from 10% to 10^{-5} while still retaining 0.5% of the signal. (The number of events in this sample is so small as to be roughly statistically independent of our overall 10σ Crab signal for the same period). This gives a 6σ result on the Crab, but with a relatively high signal to background of 1:2.3. See Figure 7. With a sample of nearly 40% gamma-rays we hope to study this to help improve further our gamma hadron separation.

2.3 Real-time Data Processing

Milagro records events at a rate of ~1700 Hz. With compression, the raw data rate is ~3.0MB/sec (~100 TB/year). When Milagro began operations in 2000, the cost and difficulties managing this quantity of data required that all raw data must be reconstructed in real time and only a subset of raw data be saved. Reconstruction consists of determining the core position, incident direction, shower size, and parameters used in gamma-hadron separation. The results of the online reconstruction are archived for every event collected; this dataset totals roughly 2 TBytes/year and is stored on two sets of redundant disk arrays (one at Los Alamos and the other at Maryland). We also have about ~10 TBytes of storage at the site, sufficient to store 6 weeks of raw data. If we or another experiment finds an interesting event we archive all raw data within 2 hours of the event time for permanent storage. In addition all raw data within 5^{o} in declination from the Crab is saved to disk. This dataset is used to test reconstruction algorithms and new gamma-hadron separation techniques. Using this Crab data we studied our reconstruction and gamma-hadron separation, but when we found improvements, as we have recently, we cannot retroactively apply these except to the Crab.

With the cost of mass storage falling, we have recently implemented a program to permanently store a larger fraction of the raw data. We have implemented this plan and are now saving all data with compactness greater than 1.2 which represents a rate about 24 TB per year. We have added another 4TB of storage at the site and are expanding our data archive at Maryland.

2.4 Energy Spectra

Without the outriggers in our data stream, it was impossible to distinguish small close by showers from large distant ones. This made determination of shower energies tenuous. Now, with the outriggers, we have made significant progress in developing accurate energy estimators. Two separate approaches have been taken: 1) Event population energy estimation and 2) Event by event energy estimation. In the former, we estimate the energy distribution based on the cuts used to select the sample. We have observed a strong correlation between our gamma/hadron separation variable, compactness, and gamma-ray energy (Figure 8). The correlation is due to the fact that gamma-ray showers with distant cores (higher energy) are less likely to have large hits in the central detector and thus a higher compactness. We can compute the spectral index of a source by fitting the slope of the compactness distribution of a measured excess. The correlation between

compactness slope and spectral index is shown in Figure 8. Using this method, we have measured the spectrum of the Crab to be 2.8 ± 0.2 (statistical error only), which, while only a preliminary result, is consistent with Crab spectrum measured by other experiments [19] . It is important to note that while this method does not directly utilize the outrigger array, it requires that the events with cores off the pond have adequate angle reconstruction, which was not available prior to the deployment of the outriggers. The second energy estimation method determines the most probable energy of each event with an estimator that includes compactness, but also event size, core position and zenith angle. This method is potentially much more accurate, but is only now being applied to data. Figure 9 (right) shows the correlation between measured and true energy for a sample of simulated gamma-rays. We expect to be able to reach ~30% energy resolution for gamma-ray showers above ~5 TeV.

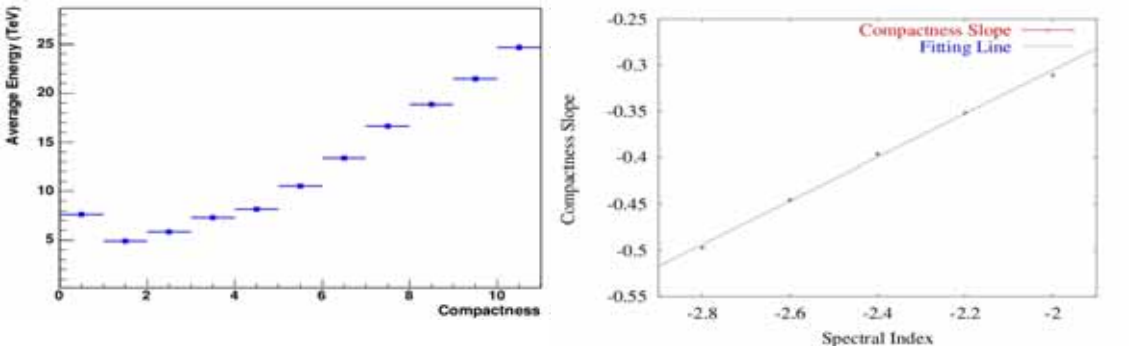

Figure 8 Energy dependence of the compactness parameter (left). The correlation between compactness slope and spectral index

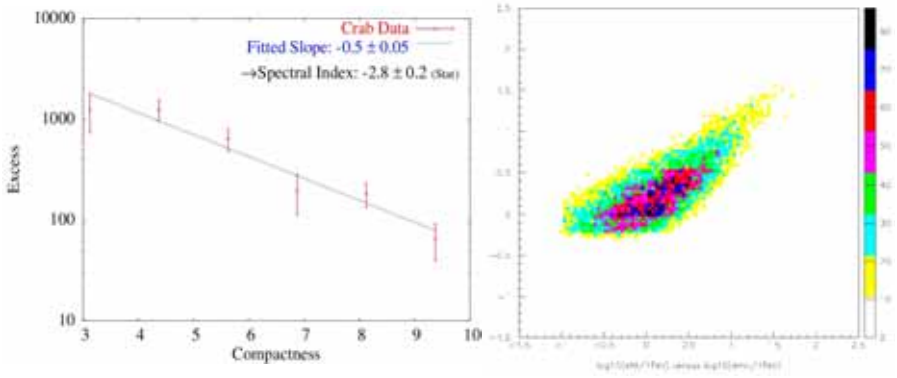

Figure 9 - The left plot shows the dependence of the crab excess on compactness. The slope of this line can be used to compute the spectral index of the crab signal. The right plot is comparison of simulated and reconstructed shower energies for individual MC events.

The statistical precision of either energy estimator depends on the observed excess from the source. Sources detected with high statistical significance will have smaller errors in the estimation of the energy spectrum. Our goal is not to develop the ability to compete with ACTs for energy spectrum measurements, but to measure the energy spectrum of the diffuse (Galactic plane) and transient (GRBs) sources which Milagro is uniquely suited to observe. We estimate that with 3 years of operation with the full outrigger array, we will

be able to measure the spectral index of the diffuse emission from the Galactic plane with a statistical error of 0.1-0.2, which is sufficient to distinguish between a hard ($\alpha \approx 2.0$-2.2) spectrum characteristic of particle acceleration regions and a soft ($\alpha \approx 2.8$) spectrum indicative of cosmic ray interactions with matter.

3 Science Results

In the past two years, the Milagro collaboration has completed construction of the outrigger array which has lead to ~1.7x increase in sensitivity to VHE gamma-ray sources through improved angular resolution and gamma/hadron separation. While doing this work, we have continued to operate at >90% ontime for collecting data. In this section we will describe our results on the search for VHE emission on all time scales from the entire overhead sky. In particular, we will highlight our results from: our all sky survey, our detection of the Galactic Plane, our study of diffuse sources, our limits on GRBs and a brief description of our solar physics results.

3.1 All-Sky Survey

Using our standard background estimation technique [20] the entire sky has been searched for excesses over the background cosmic rays using data from July. 20, 2000 to June 1, 2005. In this analysis, only the data from the online reconstruction is available. Reconstruction software that utilizes the outriggers and calibrations were only implemented online in the Fall of 2004, so the majority of the data was not reconstructed using the higher sensitivity outrigger-inclusive algorithms. In the 4.5 years of on-time collected during this period, the Crab is detected at 8.0σ using our standard cuts.

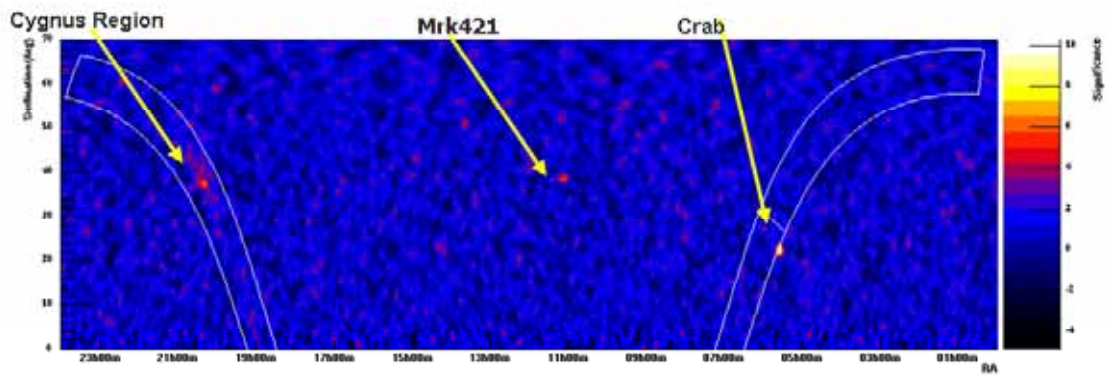

Figure 10. A significance map of the northern sky is shown using the weighted analysis. Three regions in this map show excesses over 5σ: The Crab at 10.0σ, Mrk 421 at 5.4σ and a point in the Cygnus region at 5.9σ.

We have developed a new gamma-ray source analysis in which events are weighted based on the ratio of the likelihood of the event being due to a gamma ray and the likelihood that the event is due to a hadron induced background. This weighted analysis is expected to produce a ~1.3x sensitivity improvement for a point source with the spectrum of the Crab. Note that the weights used in this analysis and the bin sizes were those found to be optimal for the old online reconstruction. For the Crab, the significance increases to 10.0σ for the 4.5y data set. A significance map of the northern sky is shown in Figure 10 using the weighted analysis. Three regions in this map show excesses over 5σ: The Crab at 10.0σ, Mrk 421 at 5.4σ and a point in the Cygnus region at 5.9σ. This result also provides a long term integrated measurement of the VHE output of Mrk 421 based on daily observations. The instantaneous luminosity of this source has been highly variable during the observation period making it difficult to estimate the total output without the continuous

monitoring provided by an instrument such as Milagro. The point in the Cygnus region of the Galactic plane is the brightest point within a larger diffuse structure which is described in detail below. Apart from these three sources, this result establishes that there are no gamma-ray point sources in the northern sky with flux greater than ~500mCrab.

3.2 Gamma Ray Bursts in Milagro

Milagro's large field of view (~2 sr) and high duty factor (>~90%) are essential for observing fast transient sources, such as gamma-ray bursts which can last only fractions of a second. The exposure of Milagro to the sky (FOV x Ontime) is roughly 4000 times higher than an ACT (4^o FOV). The GRB rate within the FOV of an ACT is only .02 GRBs/y, based on the rate of bursts detected by BATSE, while EAS arrays like Milagro observe a rate of ~100 GRBs/y within their FOV. Some VHE telescopes like MAGIC have been specifically designed to slew rapidly the location of GRBs based on notifications from satellite detectors. The problem with this approach is that fewer than 10% of GRBs are detected with prompt position information by the currently deployed array of satellite detectors. Furthermore, even with prompt notification, the time to get on the burst is typically greater than 30-40 seconds, which is much longer than the duration of the gamma-ray emission of most GRBs. With the understanding that most of the GRBs that occur in Milagro's FOV are not detected by satellites, our strategy in searching for VHE emission from GRBs is to search for emission from satellite identified GRBs that occur within Milagro's FOV and also to search for GRB's at unknown positions and times within the data set. The latter method has a lower sensitivity, due to the large number of trials incurred in the search, but does not rely on infrequent satellite coincidence.

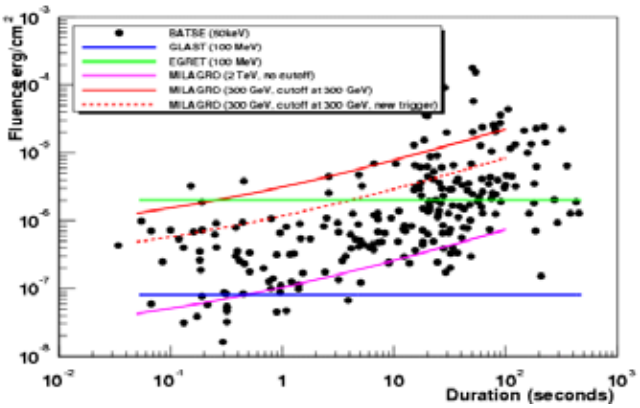

Figure 11. The sensitivity of Milagro to gamma ray bursts shown by the curved lines. The upper and lower horizontal lines are for EGRET and GLAST, respectively. The black circles show the fluence and duration for the GRBs detected by BATSE.

The number of GRBs which Milagro is expected to detect is highly uncertain and depends strongly on the fraction of GRBs which are near enough to not have the VHE emission attenuated by pair production with the infrared extragalactic background light (EBL). Models of the EBL predict that 300 GeV gamma rays can be observed up to a redshift of ~0.3-0.5. To date, 50 GRBs[21] have measured redshifts and only 5 are within $z<0.5$. If these 36 GRBs are representative of the bursts detected by BATSE which occurred at a rate of ~700 GRBs/year/(4π sr) [22] then one would expect ~ 4 GRBs/year within Milagro's field of view and with $z<0.3$ (using this observed rate of $z<0.5$ GRBs).

In the three year period from 2002-2004, after the decommissioning of CGRO, only ~90 GRBs were detected and only about 15 of these have measured redshifts. 11 of the GRBs from this period fell within Milagro's FOV and only 2 of the 11 have measured redshifts (GRB040924 with $z=0.859$ and GRB021211 with $z=1.01$). Milagro detected coincident VHE emission from none of the GRBs [23].

The Swift gamma-ray burst detector was launched in the Fall of 2004 and was became fully operational in the Spring of 2005. Swift, along with the other GRB instruments is expected to detect ~90 GRBs/year, ~25

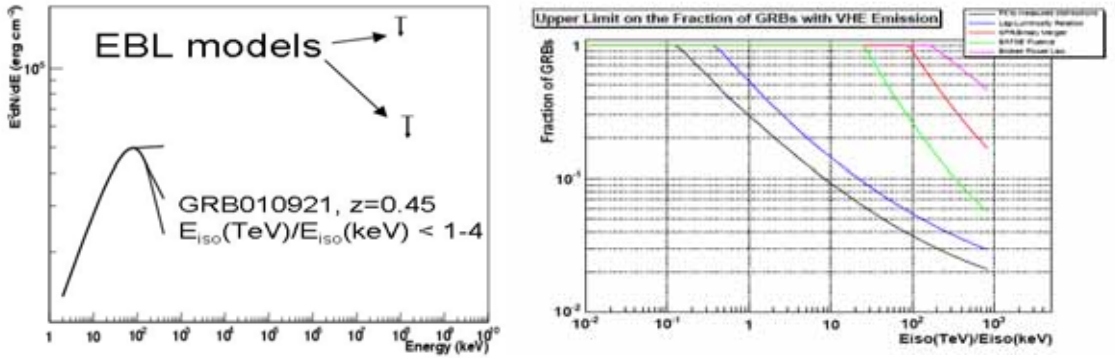

Figure 12. The left Figure shows the constraints on TeV emission for GRB010921 by Milagro's non-observation. The right Figure shows the constraints on the ratio of TeV to KeV emission for all bursts under differing assumptions of their distance distribution.

of which with measured redshifts. In the first half of 2005, 14 GRBs have already been detected to fall within Milagro's FOV. 4 of this sample have measured redshifts (GRB050319 with z=3.24, GRB050502 with z=3.793, GRB050505 with z=4.3 and GRB050509b with z=0.225). Milagro detected VHE emission from none of the GRBs in this sample. The one GRB that was close enough to possibly detect with a VHE instrument, GRB050509b, had a X-band fluence of only 2.3×10^{-8} ergs/cms^2. Milagro's 99% C.L. upper limit is 9.2×10^{-8} ergs/cm^2 in the VHE band. This GRB was one of the dimmest ever detected. A bright burst with redshift less than 0.5 within Milagro's FOV will either be detected or highly constrain GRB emission models.

Milagro also searches for short duration GRBs within our FOV unaided by satellite detectors [24]. In this "untriggered" search, the entire overhead sky is searched for transient gamma-ray sources on time scales from 250 microseconds up to 2 hours. No gamma-ray bursts have been detected by this search. However, we know that more than 200 GRBs have occurred within the FOV of the Milagro detector during this period. This result allows us to constrain the VHE output of GRBs to be less than 0.12 times the keV-MeV assuming that the VHE emission from all GRBs is a constant fraction of the keV-MeV. This constraint is highly uncertain, because it depends on models for the GRB fluence distribution, the redshift distribution of GRBs, and modeling of the extragalactic IR distribution. An alternative interpretation of this result is to place an upper limit on the fraction of GRBs with TeV emission. Figure 12 (right) shows the upper limit on the fraction of GRBs with a VHE component plotted vs. the ratio of keV-MeV and VHE fluence for several redshift models. It should be noted that all the limits presented here utilize the Primack 2004 model[25] for estimation of EBL radiation. Recent results from the HESS collaboration
indicate that the Primack model may overestimate[26] the EBL by a factor of 2. Consequently, Milagro's sensitivity is likely better than shown here.

3.3 The Galactic Plane

Diffuse emission from the galactic plane is the dominant source in the gamma-ray sky[27]. The origin of very-high-energy diffuse emission is conventionally understood to be due to the decay of π^0's produced by the interaction of cosmic-ray hadrons with interstellar matter. The flux of gamma-rays measured by EGRET below 1 GeV fits models well, while between 1 and 40 GeV models predict fluxes 60% less than that measured. It has been suggested [28] that the enhanced emission at high energies is due to inverse-Compton scattering from cosmic-ray electrons. Candidate sources for very-high-energy electrons include supernova remnants, where X-ray observations [29] of synchrotron radiation indicate the presence of electrons above

30 TeV. If cosmic-ray electron cooling and not hadronic interactions are the dominant source of diffuse gamma-ray emission from the galactic plane then, the flux might be an order of magnitude higher than previously thought at TeV energies. For this reason, ACTs have been spending an increasing amount of time searching for diffuse TeV gamma-rays from the galactic plane[30]. Milagro, because of its large aperture, high duty cycle, and good background rejection, is the world's most sensitive instrument for the detection of diffuse emission near 1 TeV.

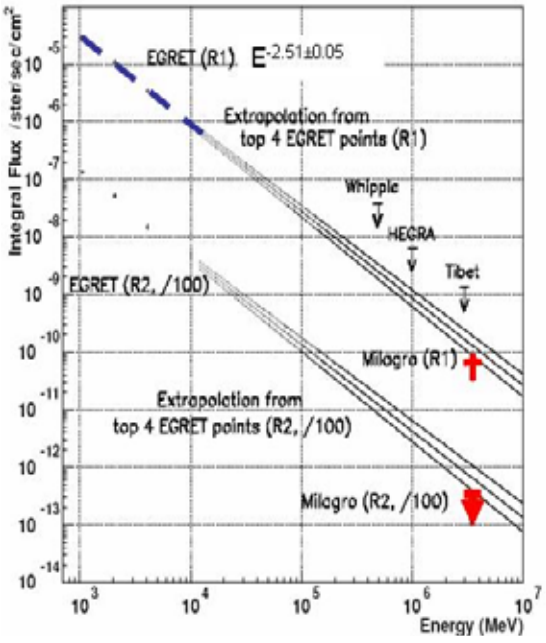

Figure 13. Milagro results on the TeV flux from the Galactic plane. The upper lines are the extrapolation of the top 4 EGRET points for the inner galaxy. Shown in red is the Milagro measurement and other upper limits. The outer galaxy is show below shifted 1/100.

Using 3 years of Milagro data beginning in July of 2000 we looked at the "inner" ($l=40^o$-100^o, $|b|<5^o$) and "outer" ($l=140^o$-220^o, $|b|<5^o$) regions of the galaxy and applied our standard gamma-hadron cut to the data. The regions were chosen *a priori* based on the distribution of the diffuse gamma-ray emission measured by EGRET. Because the signal region is so large, precise background estimation is particularly important, so for this reason we corrected for the diurnal variation of the zenith angle distribution of events [31] (due to diurnal changes in the atmosphere). The outer galaxy shows no significant excess. However, there is a 4.5σ excess in the inner galaxy. This excess of 69,800 events was detected above a background of ~238 million events taken in the region of the inner galaxy. No excess was detected from the outer Galaxy where the diffuse flux is expected to be about one third that of the inner galaxy. This result is the first detection of diffuse emission from the galactic plane and has been submitted for publication in Physical Review Letters. Previous limits set by other experiments and are shown in Figure 13. Note that the energy thresholds and fields of view differ among experiments.

3.4 Extended Sources Search

Milagro's large FOV and high duty cycle are well suited for searching for extended sources of VHE gamma-rays. We have developed a unbiased extended source all-sky search analysis by modifying our standard all-sky algorithm to search for gamma-ray sources with angular size equal to or greater than the instrument's PSF. This was done by increasing the bin size used in the standard all-sky analysis from 2.1^o (optimal for point sources) to 5.9^o in steps of 0.2^o. In total, 20 separate bin sizes are considered, each optimal for a separate candidate source size. Because the 20 separate searches are highly correlated, the trials factors are computed using MC simulations. Locations with pre-trials significance above 5σ are considered source candidates. The search was performed both using the standard Milagro analysis, and using the weighted analysis described above. In both cases, the most significant location in the sky, apart from the Crab, is an extended field coincident with the Cygnus region of the Galactic plane. With the 5.9^o bin size the Cygnus region has a significance of 9.1σ using the weighted analysis, and 6.7σ using the standard analysis. The post trials significance of the measured Cygnus region excess is 3.7σ for the standard analysis and 7.2σ for the weighted analysis. Figure 14 (left) is a significance map of the sky showing the Galactic plane.

The Cygnus region of the Galactic plane is the most luminous source of VHE gamma-rays in the northern sky, ~1.5-2 times as bright as the Crab. This result is not surprising since EGRET found the Cygnus region to be the most luminous source of GeV gamma-rays in the northern sky. The diffuse nature of the region however makes it a hard target for pointed ACTs that rely heavily on angular resolution for background separation. The Cygnus region is a complex part of the Galactic plane, so the origin of the diffuse VHE emission is not entirely clear. A large contribution must come from cosmic rays interacting with the relatively dense matter in the region which is amplified by the viewing angle, tangent to a Galactic spiral arm. The Cygnus region also contains an unidentified TeV source detected by the HEGRA telescope [32] and numerous EGRET unidentified sources [32].

Because Milagro's PSF is much smaller than the optimal bin size used to estimate the diffuse significance of the Cygnus region, we can reduce the bin size to examine the morphology of the excess. Figure 14 (right) shows the distribution of the excess in the Cygnus region convolved with the Milagro PSF. The brightest point on the map at RA=20h20m, dec=37^o is the point detected at 5.9 sigma in the all sky point source search described above. This point is also spatially coincident with 2 EGRET unidentified sources (3EG J2016+3657 and 3EG J2021+3716) and the Tibet air shower array collaboration has reported [33] this point as one of only 5 above 4 sigma in their sky surveys. Overlaid on the Milagro excess map are radio contours showing the density of neutral Hydrogen. Apart from the general localized excess within the region, there is not strong correlation between the VHE excess and the matter distribution indicating that there may be localized sources giving rise to at least some portion Cygnus region excess.

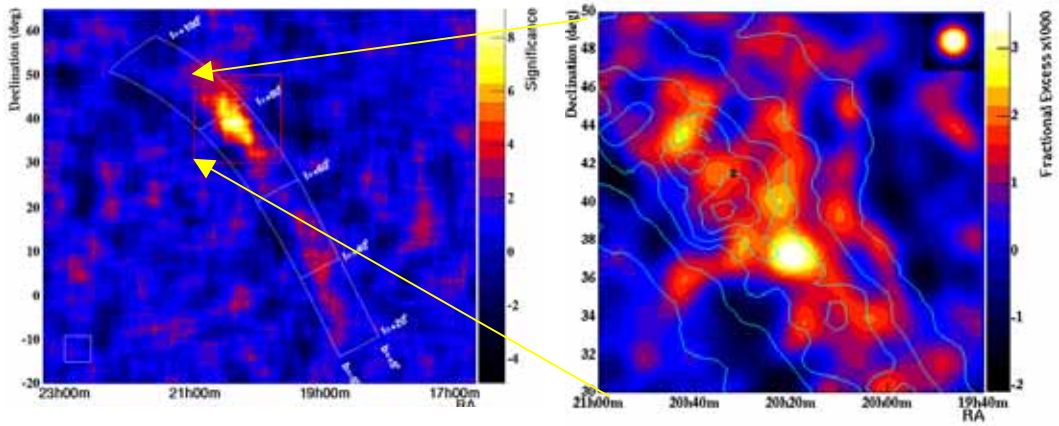

Figure 14 - Significance map of the sky showing the region of the northern sky containing the Galactic plane using a 5.9^o bin size (left) and a blowup of the Cygnus region showing the spatial distribution of the extended excess.

It is important to note that the Cygnus region excess makes a substantial contribution to the diffuse emission from the Galactic plane reported in the previous section. In this analysis, the background subtraction is not performed in a manner that allows the bin size to be expanded to be as large as the bin selected *a priori* in the Galactic plane analysis. So, to measure the contribution of the Cygnus region to the Galactic plane excess, we use a smaller bin defined as $|b|<2.0^O$, $40.0^o<l<100^o$. Using the weighted analysis, this reduced sizes galactic plane bin has an 8.0σ excess. When the Galactic longitude cut is reduced to $40.0^o < l < 75^o$ to exclude the Cygnus region, which lies roughly between l=75 and l=85, a 5.0σ excess remains. Although a substantial fraction of the diffuse Galactic plane excess is clearly due to gamma rays from the Cygnus region, a statistically significant diffuse excess lies outside the region as well. This diffuse excess is visible in the left panel of Figure 14.

3.5 Other Sources

Milagro's comprehensive maps of the gamma-ray sky allow for coincidence studies with other experiments. Milagro has searched for VHE gamma-ray excesses coincident with EGRET's catalog of unidentified sources[34]. We have also searched for emission coincident with Galaxy clusters[35], which in many cases are extended sources. The limits in both cases are the best available for most of these VHE source candidates.

3.6 Solar Physics

The sun is a prolific source of cosmic ray protons (and ions) associated with solar flares, coronal mass ejections and interplanetary shocks. In addition, the solar wind carries solar magnetic field into the interstellar medium and thereby modulates the galactic cosmic ray intensity at earth. Milagro, in its scaler mode, has detected[36] solar protons above ~10 GeV in coincidence with satellite instruments and ground-level neutron monitors. These multi-GeV protons are the result of coronal and interplanetary phenomena associated with the solar flare process. The practical "upper limit" to the acceleration of these protons has been measured to be above 10 GeV. Because of limited effective area, the maximum detectable energy for spacecraft instruments is a few hundred MeV. Using the earth's magnetic field as a magnetic spectrometer, measuring the proton spectrum from a network of neutron monitors is limited to magnetic rigidities below 15 GV (the maximum magnetic cutoff). Milagro data when combined with lower energy, complementary, neutron monitor data provides an independent measure of the cosmic-ray intensity and spectrum near the roll off of the spectrum in many events. This is important since it provides information about the acceleration (and transport) processes. As an example, Milagro detected (at $> 30\sigma$) particles from the large solar flare on 21 January 2005. Our data was in coincidence with the GOES 11 satellite. It should be noted that Milagro has much better time sampling than the satellite and can be used to study the time structure of the flare. We have recently implemented the capability to continuously monitor the coincidence rate at 8 different coincidence levels below our standard trigger threshold. This enables us to determine the high-energy part of spectrum of any detected solar event.

4 Future Plans

We plane to operate the Milagro detector for an additional 2 years (until mid 2007). During this period we will continue to refine our analysis techniques specifically for improved gamma/hadron separation and energy determination. Our recent improvements in event reconstruction make each additional year of operation roughly equivalent to 3 years of archival data. We plan to continue our studies of the diffuse emission from the Galactic plane. The improvements we have made will allow us to detect the diffuse emission with a significance greater than 10σ. Such a measurement will make it possible to measure the VHE spectrum with a statistical error as small as ~0.15 in the spectral index. Additional data may also allow us to detect diffuse emission from the anti-center of the Galaxy. We will continue to search for diffuse extended sources. Our improved sensitivity and angular resolution will allow us to map out the morphology of the diffuse excess in the Cygnus region as well as the rest of the Galactic plane. We will also be able to map out the spectrum of the Cygnus region which is important to understand the contribution from typically hard sources thought to be sites of cosmic ray acceleration and the softer more diffuse interaction of cosmic rays with matter.

Milagro is the world's best instrument capable of measuring contemporaneous VHE counterparts to GRBs. With the recent activation of the Swift satellite GRB detector, measurements from Milagro have increased importance. Since Swift can determine the redshift of a large population GRBs even upper limits from Milagro will be important in understanding gamma-ray production in GRBs. In the 3 years from 2002-2004, only 12 GRBs were detected within Milagro's FOV, and only 2 of those had measured redshifts. With Swift, we expect the number of GRBs/year detected in Milagro's FOV to more than triple to 14 and the number

with measured redshifts to increase to 4. In addition to searching for GRB counterparts with SWIFT, we will continue to perform a real-time search for TeV bursts independent of other detectors and we will alert the broader community if we detect such a burst.

4.1 HAWC/miniHAWC

We have been planning for the construction of a next generation High Altitude Water Cherenkov Experiment (HAWC). Initial design studies indicate that a high altitude (>4000m) large area water Cherenkov detector could have a threshold and sensitivity comparable to the current Whipple 10m telescope, but with 4000 times the exposure to the sky (2sr aperture, 90% on-time). Such sensitivity can be achieved by substantially increasing the size of the detector. The increase in sensitivity compared to Milagro rises much faster than the nominal square root of the rate expected from just increasing the collection area. This is possible because the lateral extent of the hadronic component of cosmic ray showers is very broad. Increasing the sensitive area of the deep layer used to identify muons and hadrons almost linearly increases the number of detected particles. Background events can be rejected with the identification of only a single penetrating particle, so a huge increase in background rejection capability is possible. HAWC simulations indicate that a large detector will be able to reject more than 99% of the hadronic background events while retaining >50% of the gamma-ray signal resulting in Q factors >~5. Milagro is only able to achieve Q factors around 1.5-2.0.

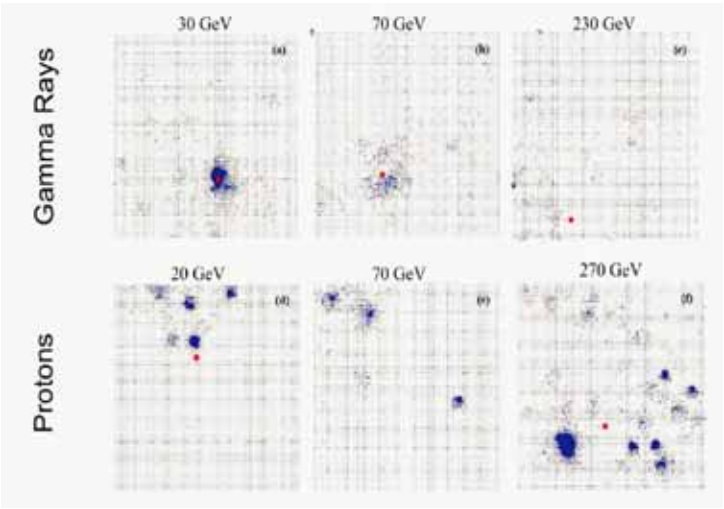

Figure 15 - Simulation of gammas and protons in HAWC.

As a low cost proof of concept for the HAWC detector, we are developing a proposal to relocate the Milagro detector PMTs and front end electronics to a high altitude site in a larger, but shallower, pond. We call this project miniHAWC. miniHAWC is expected to have a sensitivity >10x that of the Milagro detector, which is sufficient to observe the Crab during each transit at at least 4σ. The design of the miniHAWC detector is largely based on lessons learned from Milagro. In miniHAWC and HAWC, a single deep layer of PMTs is used, in contrast to the 2 layers in Milagro. A single layer with a depth of 4m is found to be a suitable substitute for both a for the 2 layers of Milagro. The PMTs are separated from each other by light tight curtains. The curtains prevent light from high energy particles from spreading beyond the cell where the energy was deposited. This innovation allows us to substantially lower the trigger threshold without incurring backgrounds from single muons. In Sept. 2005, curtains were installed in a small section of Milagro as a test of their efficacy. Preliminary results show that this reduces the number of PMTs hit by

single muon events. Rejecting muons at the trigger level allows for a much lower threshold. The current design of miniHAWC calls for a 150m x 150m x 4m covered pond. The 900 Milagro PMTs will be deployed in a 30x30 array with a separation of 5m. Figure 15 shows three typical proton and gamma induced events as viewed by the HAWC detector. Multiple large local energy deposits are visible even in very low energy hadron induced events.

Acknowledgements

We acknowledge Scott Delay and Michael Schneider for their dedicated efforts in the construction and maintenance of the Milagro experiment. This work has been supported by the National Science Foundation the USDepartment of Energy, Los Alamos National Laboratory, the University of California, and the Institute of Geophysics and Planetary Physics.

References

[1] Holder J., *et al*, 2005,"*Status and Performance of the First VERITAS Telescope*", 29th ICRC, Pune (2005)
[2] VERITAS NSF Propsoal.
[3] Baixeras, C., *et al*, Nucl. Instrum. Meth. A518 (2004) 188.
[4] Cortina J., *et al., Proc.* 29th ICRC, Pune, 5, 359 (2005).
[5] Hinton, J.A., *et al., "The Statu sof the H.E.S.S. Project",* New Astr. Rev., **48,** 131 (2004)
[6] TeV Source Catalog: http://www.icrr.u-tokyo.ac.jp/~morim/TeV-catalog.htm
[7] Meegan, C.A., *et al.,* Current BATSE gammar-ray Catalog, http://www.batse.msfc.nasa.gov
[8] Atteia, J.-L., Astrophys. J., 626 (2005) 292-297.
[9] Burrows, D. N.,*"Swift X-Ray Telescope",* astroph/0508071 (2005).
[10] Piran, T., Phys. Rep. **314** 575-667.
[11] Thompson, D. J., *et al.,* ApJS **86**, 629 (1993)
[12] Ferrer, F., astro-ph/0505414 (2005).
[13] http://glast.gsfc.nasa.gov.
[14] Dermer, C.D., Chiang, J., and Mitman, K.E., 1999, ApJ, **537**, 785.
[15] Urry, M., Astropart. Phys. 11 (1999) 159-167.
[16] Gonzalez, M.M., et al., Nature, **424**, 749 (2003).
[17] Hill, G., Highlight paper, Proc. 29th ICRC, Pune, 10, 213 (2005).
[18] Weekes, T.C., *et al*., Ap. J, **342**, 379 (1989).
[19] Aharonian, F., *et al.,* Astrophys. J., **614**, 217 (2004)
[20] Atkins, R., *et al.,* Astrophys. J. **595**, 803 (2003).
[21] Noyes, D. PhD Thesis, Univ. of Maryland Dept. of Physics 2005.
[22] Paciesas, W., *et al*., 1999, Ap J Supp **122**, 465─ 495.
[23] Atkins, R., *et al.,* Astrophys. J., **630**, 996-1002 (2005).
[24] Noyes, D., *et al.,* Proc. 29th ICRC 2005, Pune, 4, 463 (2005).
[25] Primack, J., Proceedings of the Intl. Symposium on High Energy Gamma-Ray Astronomy (2004).
[26] Hoffman, W., Highlight paper, Proc. 29th ICRC 2005, Pune, 10, 97 (2005).
[27] Hunter, S.D., *et al*., 1997, ApJ, **481**, 205.
[28] Porter, T.A. and Protheroe, R.J., 1997, J Phys G, **23**, 1765.
[29] Koyama, M., *et al*., Nature, **378**, 255 (1995).
[30] Masaki, M., Proceedings of Towards a Network of Atmospheric Cherenkov Detectors (2005).
[31] Fleysher, R.,*et al.,*Astrophys. J. **603**, 355 (2004).
[32] Hartmann, R.C, *at al*., 1999, ApJ Supp., **123**, 79.
[33] Walker, G., *et al.,* Astrophys. J., **614**, 93 (2004).
[34] Dingus, B.,*et al.,* Proc. 29th ICRC, Pune, 4, 475 (2005).
[35] Dingus, B.,*et al.,* Proc. 29th ICRC, Pune, 4, 479 (2005).
[36] Ryan, J.,*et al.,* Proc. 29th ICRC, Pune, 1, 245 and 383 (2005).